Journal of Materials Chemistry

Cite this: *J. Mater. Chem.*, 2011, **21**, 17967

www.rsc.org/materials

PAPER

Tuning the morphology of copper nanowires by controlling the growth processes in electrodeposition

Sangwoo Shin,[a] Beom Seok Kim,[a] Kyung Min Kim,[a] Bo Hyun Kong,[b] Hyung Koun Cho[b] and Hyung Hee Cho*[a]

Received 6th September 2011, Accepted 15th September 2011
DOI: 10.1039/c1jm14403k

We present an alternative route to fabricate Cu nanowires having various classes of morphologies by controlling the deposition temperature. A rough nanowire with an irregular wire diameter along the wire axis is obtained at a high deposition temperature, whereas a smooth, compact nanowire is obtained as the temperature is lowered. However, as the temperature is dropped further down to subzero degrees, an unusual behavior is observed where the nanowires exhibit rough, dendritic morphologies with relatively uniform wire diameters. We explain this peculiar growth behavior on the basis of kinetic and thermodynamic growth processes.

Introduction

In the last decade, nanowires have attracted a considerable amount of attention, especially in the fields of electronics and energy applications because of their unique transport properties.[1,2] The transport properties of a nanowire can be tuned *via* several approaches including control of the nanowire geometry[3–6] and introduction of artificial nanostructures.[7,8] Because surface effects are an important feature in nanowires, a simple and effective method for modifying the transport properties of a nanowire is to vary the surface morphology.[9–12]

Using the electrodeposition technique, the surface morphology of a nanowire can be easily modified. Among many fabrication methods, template-assisted electrodeposition is regarded as an attractive route for the synthesis of nanowire arrays because of its simplicity, cost-effectiveness, room-temperature fabrication, *etc.*[13,14] In electrodeposition, the morphology of a deposit is affected by various factors such as the overpotential, concentration, temperature, pH, and additives.[15,16] For instance, when the concentration of the electrolyte is high, existing grains are preferentially grown into larger grains whereas a large number of small grains and nuclei are formed when the concentration of the electrolyte is low.[16] This behavior can also be applied to overpotential, pH, and temperature where increased overpotential, pH, and temperature may lead to larger grains and less nucleation density, and *vice versa*.[15,16] Among the aforementioned factors, temperature is a simple but peculiar factor that significantly affects the morphology *via* controlling the growth processes.

In this study, we present a temperature-dependent morphological change of electrodeposited Cu nanowires. Besides the well-known behavior on the temperature-dependent morphological change, an unusual morphology is obtained at a very low deposition temperature which opposes the general explanation. Although not clearly understood, we explain this intriguing behavior on the basis of various growth processes.

Experimental

For the electrodeposition of Cu nanowires, commercially available AAO (Anodisc™, nominal pore size 20 nm, Whatman) with a thickness of approximately 60 μm was used as a template. The aqueous Cu electrolyte consisted of 220 g L^{-1} (0.88 M) $CuSO_4 \cdot 5H_2O$ (99%) and 32 g L^{-1} (0.33 M) H_2SO_4 (95%) in deionized water (18.2 MΩ cm). All of the chemicals used in the present study were purchased from Duksan Pure Chemicals (Seoul, Korea) and were used as received without further purification.

A three-electrode electrochemical cell was employed for Cu electrodeposition. A 300 nm Au film with a 20 nm Cr adhesion layer was coated on one side of the template (narrow pore end) using an e-beam evaporator as the working electrode. Ag/AgCl (saturated KCl) and Pt mesh electrodes were used as the reference and counter electrode, respectively. The optimal reduction potential was determined by linear voltammetry and was set to 50 mV (*vs.* standard hydrogen electrode) during potentiostatic electrodeposition.[17] The potential was given in relation to the standard hydrogen electrode (SHE) because the potential of the Ag/AgCl electrode is highly temperature dependent.[18] To calibrate the temperature effect, a linear temperature coefficient of the Ag/AgCl electrode *versus* SHE was given as −1.01 mV K^{-1}.[18] Linear voltammetry and potentiostatic electrodeposition were carried out using a standard potentiostat (VersaSTAT3, Princeton Applied Research). Using a constant temperature

[a]*Department of Mechanical Engineering, Yonsei University, Seoul, 120-749, Korea. E-mail: hhcho@yonsei.ac.kr; Fax: +82 2 312 2158; Tel: +82 2 2123 2828*
[b]*School of Advanced Materials Science and Engineering, Sungkyunkwan University, Suwon, Gyeonggi-do, 440-746, Korea*

circulating bath (HI-1030I, Hanil), the deposition temperature was varied from −1.5 to 60.5 °C and precisely maintained at a deviation of ±0.1 °C.

To obtain TEM images (JEM-3010, JEOL), samples of individual nanowires were prepared by dissolving the AAO template in 1 M NaOH for 1 day, thoroughly rinsing with absolute ethanol, and sonicating for 10 min.

Owing to the presence of narrowing features at both ends of the template,[17] approximately 10 μm of the template was removed with a mechanical polisher, and the exact pore diameters of the AAO templates were observed *via* SEM (S-4300, Hitachi).

Results and discussion

Scheme 1 shows schematic illustration of a typical electrodeposition process at an atomistic scale. Blue, green, and yellow particles represent metal ions, adatoms, and stable atoms, respectively. Note that in the present study, all the surface movements of the adatoms including intralayer and interlayer transport are regarded as a single term 'surface diffusion.' The electrodeposition of nanowire is progressed in the following order: metal ions from the bulk electrolyte are transported and reduced to the surface by bulk diffusion and migration. The rate of this process is determined by the growth kinetics (green arrow in Scheme 1(a)).[19] Adatoms are then diffused toward energetically more favorable sites which is a thermodynamic process (blue arrow in Scheme 1(a)).[19]

The rate of these processes can be simply controlled by varying the temperature because all of the processes that occur during the electrodeposition (bulk diffusion, migration, and surface diffusion) are determined by individual diffusion coefficients that directly follow the Arrhenius equation.[20] Thus, by controlling the temperature, competition between the two growth processes (*i.e.*, kinetics and thermodynamics) can be varied. Because the morphology of a deposit is affected by different growth processes, morphological changes can be induced by controlling the competition between the individual processes.[16]

In general, when the deposition temperature is high, the surface diffusion of adatoms is enhanced, which favors the growth of preexisting grains and nuclei, leading to coarse crystallites that result in a rough surface morphology.[15,17] In contrast, low deposition temperature suppresses the preexisting grain growth, allowing a large number of new nuclei to be simultaneously formed. Thus, fine and compact grains are formed, which lead to a relatively smooth surface morphology. This temperature-dependent behavior of the surface morphology has been widely observed in previous studies including nanowires[15,21–24] and thin films[25–31] as well as in this study.

Fig. 1 presents the TEM images of the nanowires fabricated at various deposition temperatures. These images clearly show that the nanowires grown at different temperatures exhibit different morphologies and sizes. At 5.2 °C, the nanowires exhibit a smooth and compact morphology with uniform wire diameter along the wire axis (Fig. 1(f)–(j)) because of the fine grains formed at low deposition temperature. The ring pattern in the electron diffraction (ED) patterns, shown in the inset of Fig. 1(f), is a direct indicative of enhanced polycrystallinity due to the fine grains. Compact pore filling can be confirmed by analyzing the diameter distribution of the nanowires. Because the diameter of the nanowire is obviously limited by the pore geometry, pore filling can be easily verified by comparing the diameter distribution of nanowires to the template pores. As shown in Fig. 2(b), nanowires grown at 5.2 °C present an average diameter of

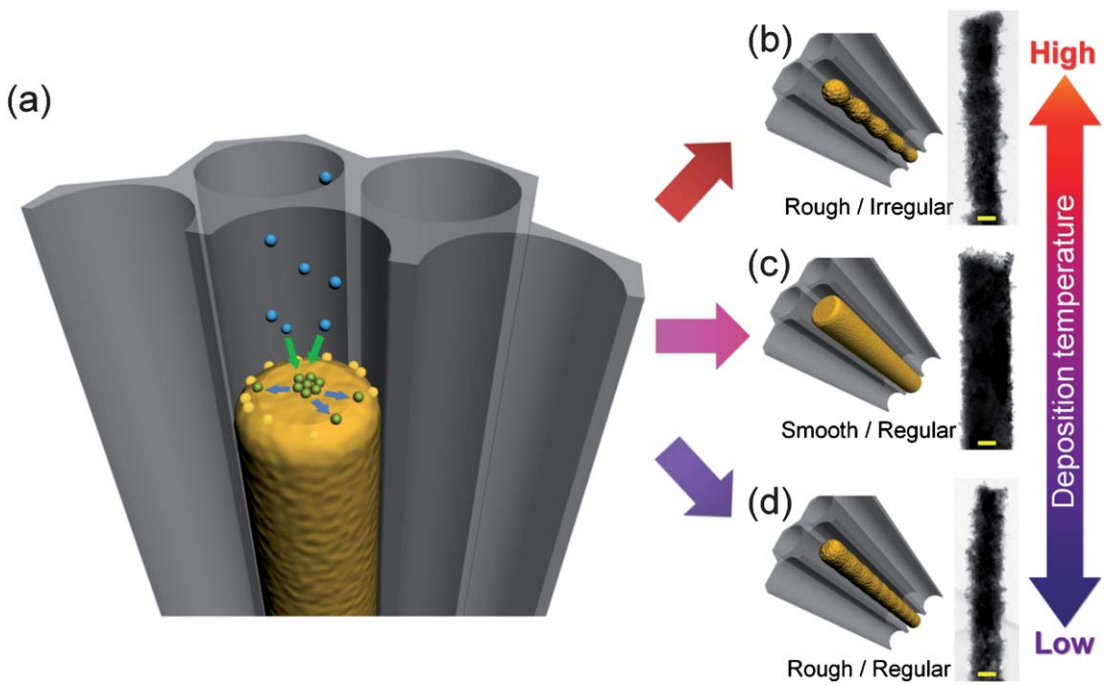

Scheme 1 Schematic depiction of nanowire electrodeposition at various temperatures. In (a), blue, green, and yellow particles represent ions, adatoms, and stable atoms, respectively, and green and blue arrows represent ion diffusion and surface diffusion. Scale bars for the inset TEM images in (b–d) are all 100 nm.

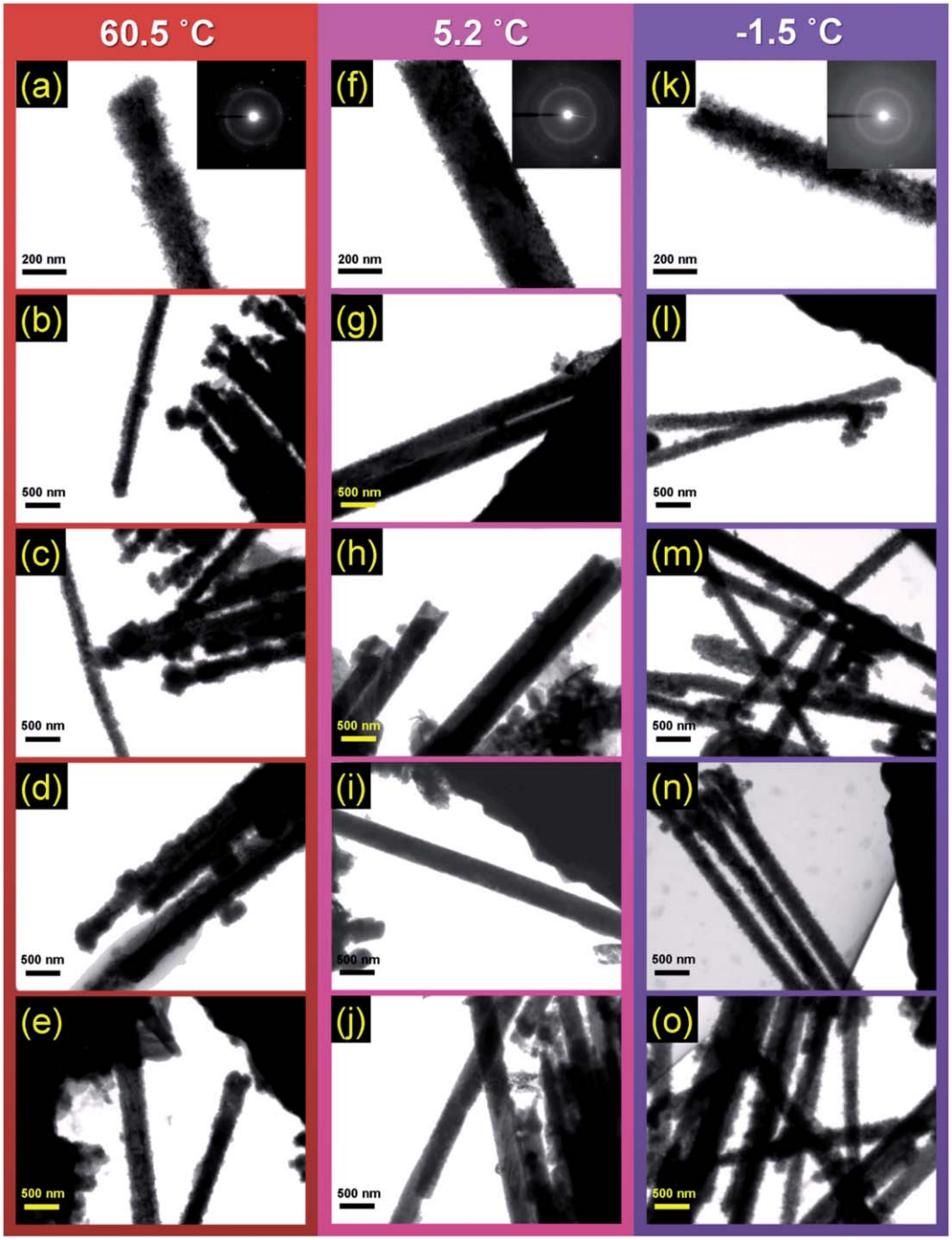

Fig. 1 TEM images of the Cu nanowires grown at different temperatures: (a–e) 60.5 °C; (f–j) 5.2 °C; and (k–o) −1.5 °C. The insets in (a), (f), and (k) indicate electron diffraction patterns.

approximately 327.5 nm, and the corresponding diameter distribution pattern nearly overlaps the pore distribution of the template, indicating that the complete pore filling is achieved. Moreover, additional surface diffusion of the adatoms should favor more smooth and compact morphology. This process is more of a thermodynamically controlled process under specific growth conditions where the ions are diffused and reduced toward the growth front at an appropriate rate that is favorable to the complete pore filling.[19] Therefore, a relatively smooth and compact nanowire with a large wire diameter that is limited by the pore size was obtained (Scheme 1(c)).

As the deposition temperature is increased up to 60.5 °C, the nanowires exhibit a very rough morphology with an irregular wire diameter along the wire axis (Fig. 1(a)–(e)). This is mainly due to the rapid ion transfer and nuclei growth where the accelerated growth kinetics as well as thermodynamics due to the elevated temperature promotes rapid nanowire growth at rates up to 750 nm s^{-1} and the instantaneous growth of preexisting

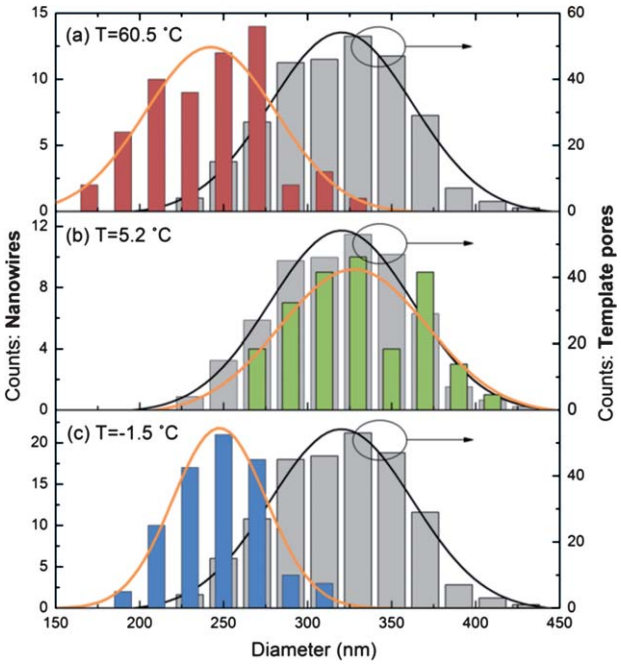

Fig. 2 Diameter histograms of the electrodeposited Cu nanowires at various temperatures: (a) 60.5 °C; (b) 5.2 °C; and (c) −1.5 °C. The orange curves are fits to the Gaussian function. Gray bars and black Gaussian fit are from the partially polished AAO template.

nuclei (please refer to Fig. 2(b) in ref. 17). The enhanced growth of grains can be confirmed by the ED results (Fig. 1(a)). Compared to nanowires grown at lower temperatures, more diffraction spots are observed in the nanowires grown at 60.5 °C (Fig. 1(f)), which is an indicative of enhanced crystallinity.

Also, when the nanowire growth is fast, it is likely to occur even before the surface diffusion is fully progressed, incoming ions are rapidly reduced onto the surface, which hinders the surface diffusion of preexisting adatoms by providing an additional cohesive energy.[15] Moreover, rapid ion transport toward the growth front of existing grains inhibits the growth of new nuclei and formation of grains that compactly fill the pores of the template. This rapid growth process should lead to nanowires with rough surface morphologies and irregular wire diameters. As shown in Fig. 2(a), the size distribution of nanowires exhibits a broad distribution with much smaller average diameter (247.6 nm) compared to the template pores (320.1 nm). Therefore, despite the high temperature, and owing to the rapid nanowire growth, this process can be regarded as a kinetic-driven growth process that can result in a rough surface morphology with irregular wire diameter (Scheme 1(b)).

An intriguing result comes from the lowest temperature data at −1.5 °C where the TEM images show rough dendritic surface morphologies with small wire diameters. Opposing from the general explanation, this unusual behavior is not well understood and has not been observed previously to the best of our knowledge. Nevertheless, such unclear behavior should also be an outcome of competition between kinetics and thermodynamics.[15,19]

When the deposition temperature is very low, the growth kinetics are greatly hindered due to the decreased ion diffusion where the nanowire growth rate is shown to be as low as about 50 nm s^{-1}.[17] This slow kinetic process inhibits pore filling of the ions and adatoms that results in a small wire diameter because the adatoms should be mainly concentrated in the central region of the pore rather than completely filling the pore. Previous reports on Fe nanowires prove that when the ions are insufficiently supplied *via* lowering the ion concentration, the growth rate along the channel direction exceeded the lateral growth rate, which resulted in an incomplete pore filling thereby having a rough surface morphology and smaller nanowire diameter.[32,33] The insufficient supply of ions is essentially an ion depletion in the diffusion layer under a diffusion-limited environment, and it is well known that long and narrow pores of the AAO template having an aspect ratio greater than 100 exhibit a diffusion-limited behavior.[17,32]

In addition, as the temperature is decreased further down to −1.5 °C, the thermodynamics is shown to be significantly hindered, which should result in the further suppression of grain growth that eventually leads to an amorphous-like material. This is confirmed through the blurry image of the ED patterns and the spotty TEM images (Fig. 1(k)–(o)). Note that Dou *et al.* recently predicted that an amorphous nanowire would be obtained if the growth process was completely controlled by kinetics[19] and our results show that the thermodynamics are significantly hindered at −1.5 °C.

Under a thermodynamically nonequilibrium state, adatoms are less likely to diffuse away to more favorable sites such as step edges and kinks because they do not have enough energy to overcome the energy barriers, such as surface diffusion barrier and Ehrlich-Schwoebel (step-edge) barrier.[19,34] The energy barrier for the surface diffusion of Cu adatoms (~1 eV for (111))[35] is generally several times larger than that of Cu ion diffusion (~0.2 eV);[36] thus, surface diffusion is more temperature dependent than ion diffusion. Therefore, owing to the suppressed growth kinetics and thermodynamics, the pores are incompletely filled, which results in the formation of a gap between the nanowire and the pore wall. As a result, a free surface is formed at the walls of the nanowires, which promotes a rough, dendritic surface morphology.

As shown in Fig. 2(c), the average diameter of the nanowires (242.3 nm) is significantly smaller than the average pore diameter (320.1 nm), owing to the incomplete pore filling. The average diameter is nearly identical to that of nanowires grown at 60.5 °C; however, a narrower distribution is observed, indicating that the nanowires present a more uniform wire diameter. Owing to the suppressed growth kinetics and thermodynamics, a rough nanowire with a relatively small diameter was successfully obtained even at a low deposition temperature.

One may possibly suggest that the unusual morphology and size variation may be due to the thermal expansion of the template under the broad temperature range. However, the thermal expansion coefficient of AAO is relatively low (~7.7×10^{-6} K^{-1}),[37] and this leads to an overall strain change of about 0.05% across the entire temperature range. As a result, this creates the maximum deformation of only about 0.15 nm in a 300 nm pore. Therefore, thermal expansion is unlikely to control the morphology and size of the nanowire; the growth behavior observed in the present study is likely the outcome of competition between kinetics and thermodynamics.

Conclusions

In summary, we have successfully fabricated nanowires with various morphologies by changing the temperature and controlling the rates of two different growth mechanisms, *i.e.* kinetics and thermodynamics. These artificially modified morphologies may suggest a new possibility to be utilized in various technological applications. For instance, smooth and compact nanowires can be considered as a potential application for interconnects in nanoelectronics, and rough nanowires can be applied to energy-related applications. In photovoltaics, an enlargement in the surface area of nanowires *via* artificial roughening effectively increases the output efficiency.[12,38] Also, in thermoelectric, rough nanowires are employed to effectively scatter phonons, which significantly increases the thermoelectric figure of merit.[9] When utilized in phase-change memory devices, a reduction in the thermal conductivity may lead to joule heat confinement, which reduces the energy consumption.[39] Moreover, an enlargement in the surface area of nanowires due to a rough surface morphology is favorable for efficient heat transfer applications, especially boiling heat transfer.[40]

Acknowledgements

This work was supported by the National Research Foundation of Korea (NRF) grant funded by the Korea government (MEST) (no. 2011-0000252 and no. 2011-0017673).

Notes and references

1 A. I. Hochbaum and P. Yang, *Chem. Rev.*, 2010, **110**, 527.
2 P. Yang, R. Yan and M. Fardy, *Nano Lett.*, 2010, **10**, 1529.
3 Z. Zhang, X. Sun, M. S. Dresselhaus, J. Y. Ying and J. Heremans, *Phys. Rev. B: Condens. Matter Mater. Phys.*, 2000, **61**, 4850.
4 Y. Tian, G. Meng, S. K. Biswas, P. M. Ajayan, S. Sun and L. Zhang, *Appl. Phys. Lett.*, 2004, **85**, 967.
5 D. Li, Y. Wu, P. Kim, L. Shi, P. Yang and A. Majumdar, *Appl. Phys. Lett.*, 2003, **83**, 2934.
6 A. I. Boukai, Y. Bunimovich, J. Tahir-Kheli, J.-K. Yu, W. A. Goddard, III and J. R. Heath, *Nature*, 2008, **451**, 168.
7 M. S. Gudiksen, L. J. Lauhon, J. Wang, D. C. Smith and C. M. Lieber, *Nature*, 2002, **415**, 617.
8 M. T. Björk, B. J. Ohlsson, T. Sass, A. I. Persson, C. Thelander, M. H. Magnusson, K. Deppert, L. R. Wallenberg and L. Samuelson, *Appl. Phys. Lett.*, 2002, **80**, 1058.
9 A. I. Hochbaum, R. Chen, R. D. Delgado, W. Liang, E. C. Garnett, M. Najarian, A. Majumdar and P. Yang, *Nature*, 2008, **451**, 163.
10 R. Chen, A. I. Hochbaum, P. Murphy, J. Moore, P. Yang and A. Majumdar, *Phys. Rev. Lett.*, 2008, **101**, 105501.
11 P. Martin, Z. Aksamija, E. Pop and U. Ravaioli, *Phys. Rev. Lett.*, 2009, **102**, 125503.
12 S. H. Ko, D. Lee, H. W. Kang, K. H. Nam, J. Y. Yeo, S. J. Hong, C. P. Grigoropoulo and H. J. Sung, *Nano Lett.*, 2011, **11**, 666.
13 T. M. Whitney, J. S. Jiang, P. C. Searson and C. L. Chien, *Science*, 1993, **261**, 1316.
14 A. Eftekhari, *Nanostructured Materials in Electrochemistry*, Wiley-VCH Verlag GmbH & Co. KGaA, Weinhein, 2008.
15 M. Tian, J. Wang, J. Kurtz, T. E. Mallouk and M. H. W. Chan, *Nano Lett.*, 2003, **3**, 919.
16 D. Grujicic and B. Pesic, *Electrochim. Acta*, 2002, **47**, 2901.
17 S. Shin, B. H. Kong, B. S. Kim, K. M. Kim, H. K. Cho and H. H. Cho, *Nanoscale Res. Lett.*, 2011, **6**, 467.
18 D. T. Sawyer, A. Sobkowiak and J. L. Roberts, *Electrochemistry for Chemists*, John Wiley and Sons, New York, NY, 2nd edn, 1995.
19 X. Dou, G. Li and H. Lei, *Nano Lett.*, 2008, **8**, 1286.
20 H. Natter and R. Hempelmann, *J. Phys. Chem.*, 1996, **100**, 19525.
21 M. E. Toimil-Molares, V. Buschmann, D. Dobrev, R. Neumann, R. Scholz, I. U. Schuchert and J. Vetter, *Adv. Mater.*, 2001, **13**, 62.
22 K. M. Razeeb and S. Roy, *J. Appl. Phys.*, 2008, **103**, 084302.
23 M. E. Toimil-Molares, J. Brötz, V. Buschmann, D. Dobrev, R. Neumann, R. Scholz, I. U. Schuchert and J. Vetter, *Nucl. Instrum. Methods Phys. Res., Sect. B*, 2001, **185**, 192.
24 I. Hanzu, T. Djenizian, G. F. Ortiz and P. Knauth, *J. Phys. Chem. C*, 2009, **113**, 20568.
25 C. K. Chung, W. T. Chang, C. F. Chen and M. W. Liao, *Mater. Lett.*, 2011, **65**, 416.
26 J. Garcia-Torres, E. Vallés and E. Gómez, *Electrochim. Acta*, 2010, **55**, 5760.
27 U. Sahaym, S. L. Miller and M. G. Norton, *Mater. Lett.*, 2010, **64**, 1547.
28 S. Ban and S. Maruno, *Biomaterials*, 1995, **16**, 977.
29 P. E. de Jongh, D. Vanmaekelbergh and J. J. Kelly, *Chem. Mater.*, 1999, **11**, 3512.
30 F. J. Fabri Miranda, O. E. Barcia, S. L. Diaz, O. R. Mattos and R. Wiart, *Electrochim. Acta*, 1996, **41**, 1041.
31 A. Goux, T. Pauporté, J. Chivot and D. Lincot, *Electrochim. Acta*, 2005, **50**, 2239.
32 H. Schlörb, V. Haehnel, M. S. Khatri, A. Srivastav, A. Kumar, L. Schultz and S. Fähler, *Phys. Status Solidi B*, 2010, **247**, 2364.
33 V. Haehnel, S. Fähler, P. Schaaf, M. Miglierini, C. Mickel, L. Schultz and H. Schlörb, *Acta Mater.*, 2010, **58**, 2330.
34 S.-C. Li, Y. Han, J.-F. Jia, Q.-K. Xue and F. Liu, *Phys. Rev. B: Condens. Matter Mater. Phys.*, 2006, **74**, 195428.
35 P. Wynblatt and N. A. Gjostein, *Surf. Sci.*, 1968, **12**, 109.
36 M. S. Moats, J. B. Hiskey and D. W. Collins, *Hydrometallurgy*, 2000, **56**, 255.
37 X. J. Xu, G. T. Fei, W. H. Yu, L. Chen, L. D. Zhang, X. Ju, X. P. Hao and B. Y. Wang, *Appl. Phys. Lett.*, 2006, **88**, 211902.
38 J. Weickert, R. B. Dunbar, H. C. Hesse, W. Wiedemann and L. Schmidt-Mende, *Adv. Mater.*, 2011, **23**, 1810.
39 H. Tanaka, T. Nishihara, T. Ohtsuka, K. Morimoto, N. Yamada and K. Morita, *Jpn. J. Appl. Phys.*, 2002, **41**, L1443.
40 R. Chen, M.-C. Lu, V. Srinivasan, Z. Wang, H. H. Cho and A. Majumdar, *Nano Lett.*, 2009, **9**, 548.